

# Supplementary Information: Modelling and correcting the impact of RF pulses for continuous monitoring of hyperpolarized NMR

Gevin von Witte<sup>1,2</sup>, Matthias Ernst<sup>2</sup>, Sebastian Kozerke<sup>1\*</sup>

<sup>1</sup>University and ETH Zurich, Institute for Biomedical Engineering, Zurich 8092, Switzerland

<sup>2</sup>ETH Zurich, Laboratory of Physical Chemistry, Zurich 8093, Switzerland

\*author: kozerke@biomed.ee.ethz.ch

This document is structured into three sections: The first two deal with the simulated performance of the three discussed methods to correct for the readout RF pulses. The last section shows an experimental (uncorrected) FID to support the signal-to-noise ratio (SNR) discussion of the main text.

For the assessment of the three corrections ( $1/\cos^n$ , CC-model as introduced in [1] and our newly introduced iterative, self-consistent correction) in the simulations, we used a time slicing approach to numerically integrate Eq. 1 of the main paper with RF pulses applied at a fixed repetition time  $T_R$ . The simulations included a large noise (compare SNR in the simulations for  $2.5^\circ$  pulses with the experimental FID shown in Fig. S14 with an SNR of around 1000 based on the first data point of the FID). The build-ups and decay observed with noise and RF pulses can show very distinct apparent hyperpolarization dynamics compared to the assumed experimental parameters (compare Figs. 1a and S6 as well as Tab. 1 and S1). The discussed corrections were then applied to these apparent build-ups and decays and the results of the corrections can be compared with the expectations (indicated as horizontal lines in the figures below) based on the assumed experimental parameters. Specifically, the figures below show how the iterative, self-consistent correction converges with the number of iterations (fitting of the build-up/ decay data and correcting the data with the fitted time constant, see main text for more information) as well as a statistical analysis of the corrections for simulated data for all three correction methods.

## S1 Simulations of noisy build-ups with RF pulses

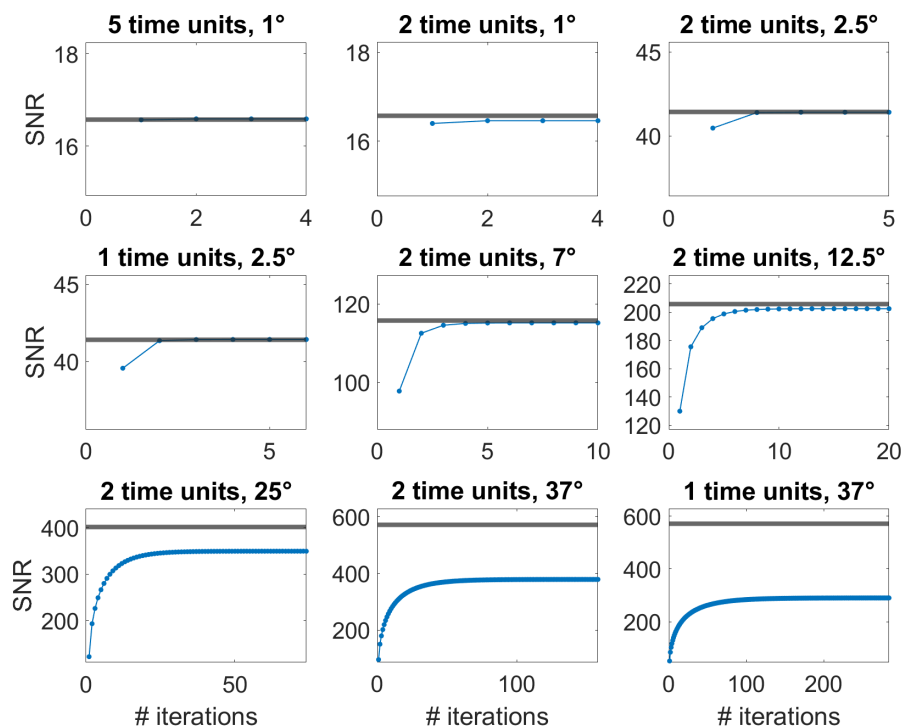


**Fig. S1.** Simulating the convergence of  $\tau_{\text{bup}}$  in the self-consistent algorithm for synthetic experimental (noisy) data for different RF pulse settings. Assumed experimental parameters without pulses:  $P_0 = 0.3$ ,  $\tau_{\text{bup}} = 50$ ,  $A = 1$

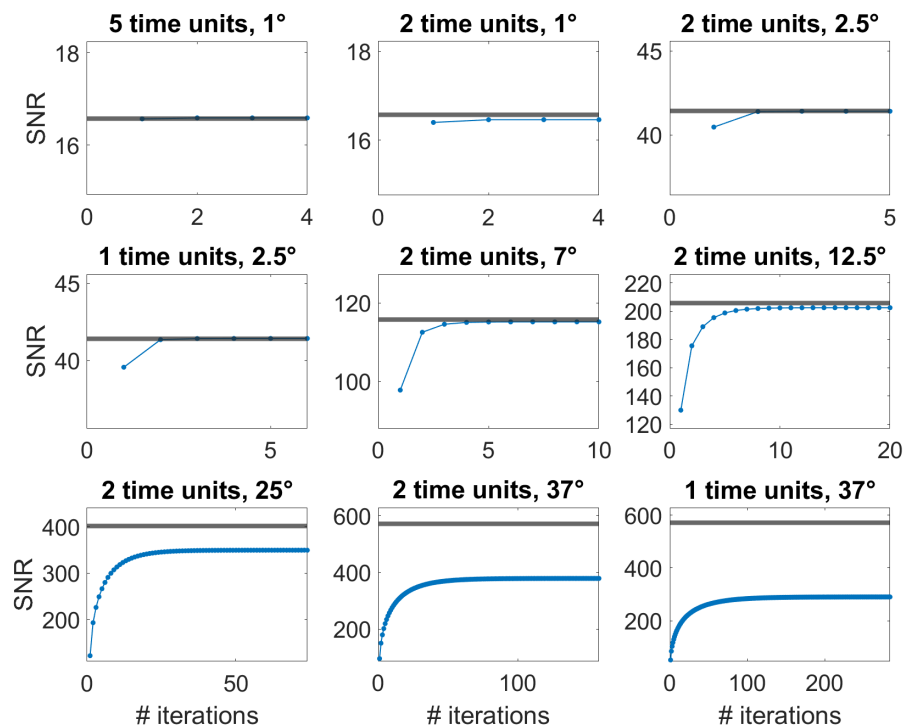


**Fig. S2.** Simulating the convergence of the SNR and with it the polarization in the self-consistent algorithm for synthetic experimental (noisy) data for different RF pulse settings. Assumed experimental parameters without pulses:  $P_0 = 0.3$ ,  $\tau_{\text{bup}} = 50$ ,  $A = 1$

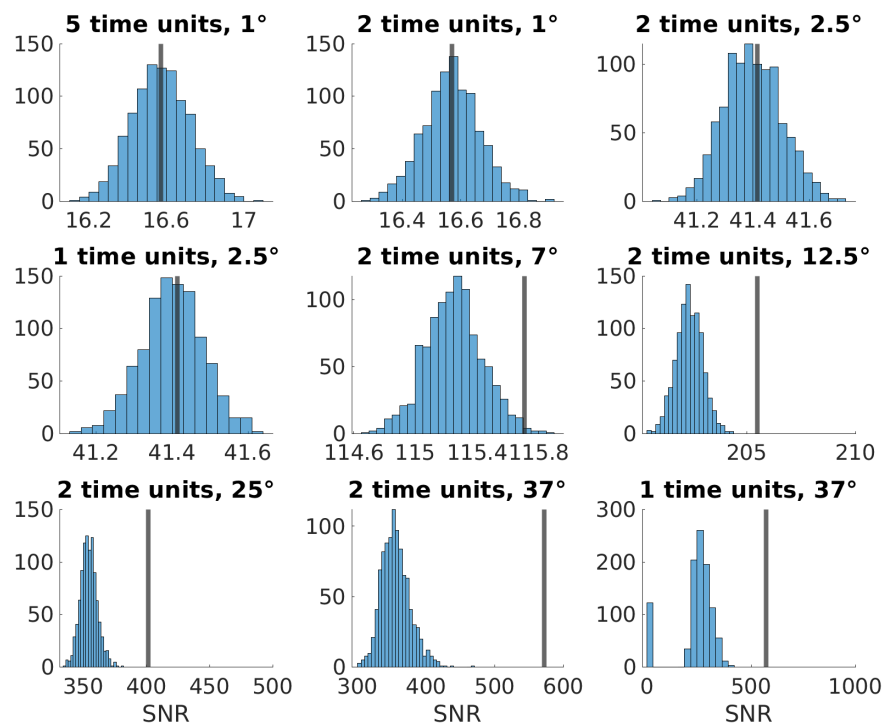


**Fig. S3.** Results of the iterative self-consistent correction algorithm for the (SNR) with different RF schemes. Assumed experimental parameters without pulses:  $P_0 = 0.3$ ,  $\tau_{\text{bup}} = 50$ ,  $A = 1$ , 1000 configurations with a maximum of 500 self-consistent iterations each. The results with zero SNR refer to cases in which the algorithm could not find a self-consistent solution for the given convergence criterion (less than  $10^{-4}$  time units difference for the time constant between consecutive iteration steps).

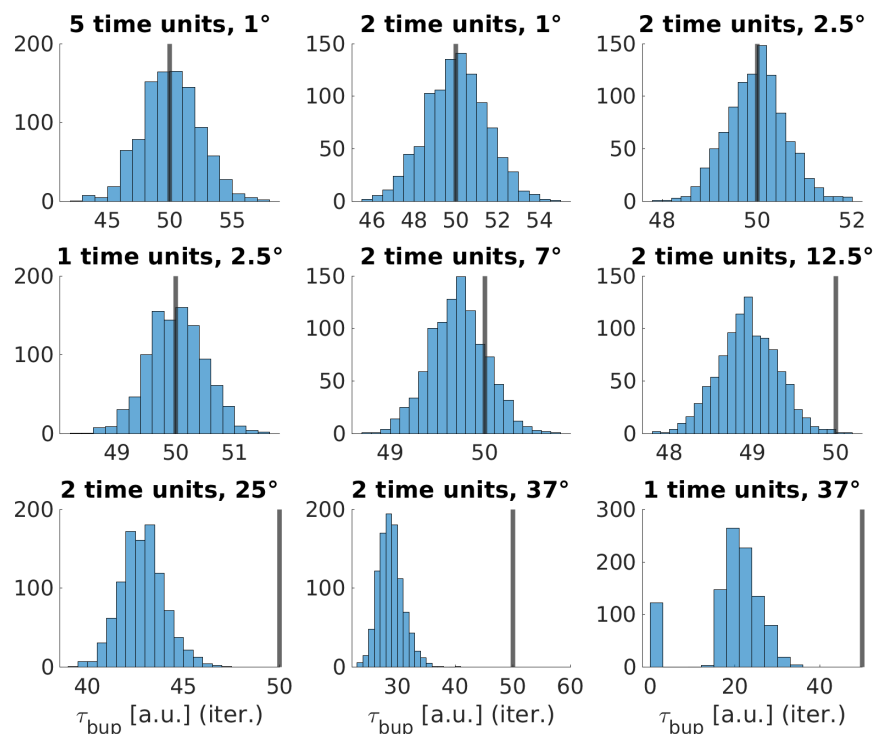


**Fig. S4.** Results of the iterative self-consistent correction algorithm for the build-up time constants with different RF schemes. Assumed experimental parameters without pulses:  $P_0 = 0.3$ ,  $\tau_{\text{bup}} = 50$ ,  $A = 1$ , 1000 configurations with a maximum of 500 self-consistent iterations each. The results with zero build-up time refer to cases in which the algorithm could not find a self-consistent solution for the given convergence criterion (less than  $10^{-4}$  time units difference for the time constant between consecutive iteration steps).

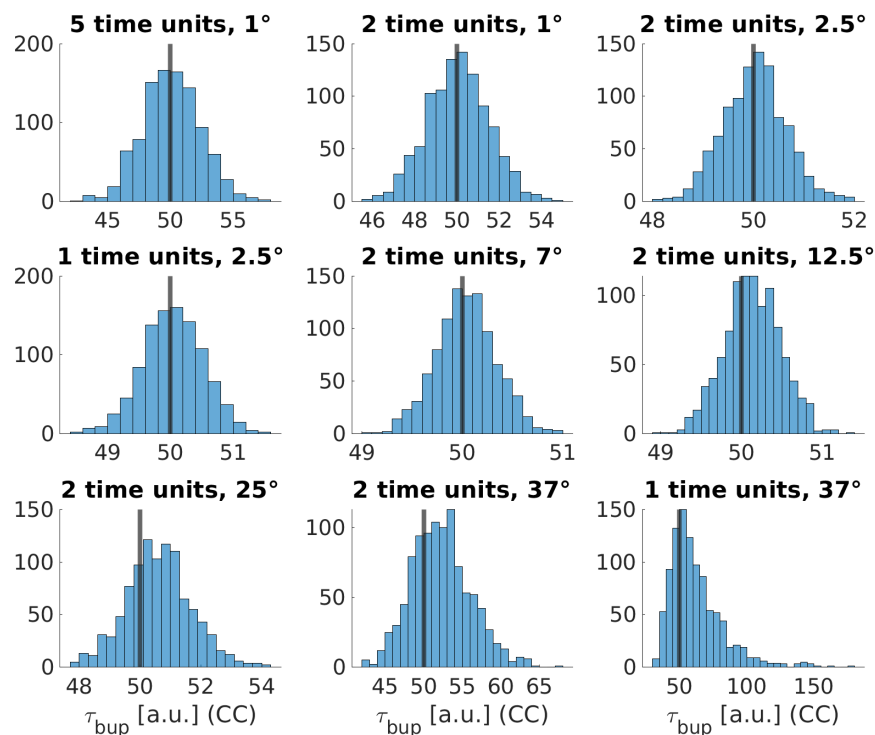


**Fig. S5.** Results of build-up time correction introduced in [1] (CC model). Assumed experimental parameters without pulses:  $P_0 = 0.3$ ,  $\tau_{\text{bup}} = 50$ ,  $A = 1$ , 1000 configurations.

## S2 Simulations of noisy decays with RF pulses

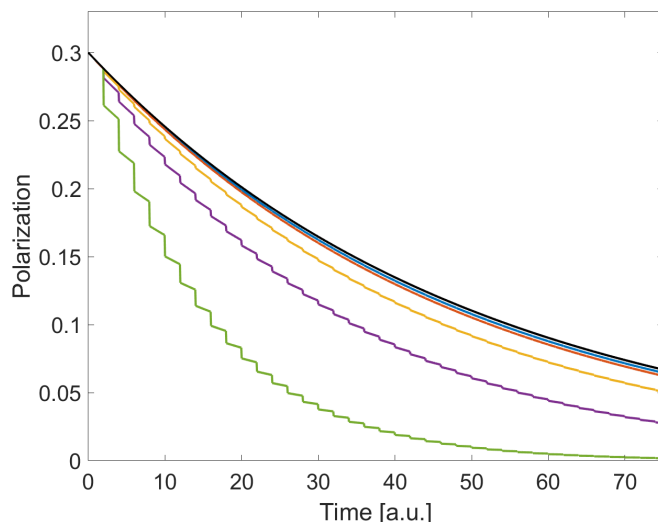


**Fig. S6.** (Main plot) Comparison of decays under the influence RF pulses without noise. The black curve is without RF pulses. The RF scheme for the other curves (from top to bottom):  $2.5^\circ$ , 2 time units;  $2.5^\circ$ , 1 time unit;  $7^\circ$ , 2 time units;  $12.5^\circ$ , 2 time units;  $25^\circ$ , 2 time units. Assumed experimental parameters without pulses:  $P_0 = 0.3$ ,  $\tau_{\text{decay}} = 50$

Flip angle [°]	2.5	2.5	7	12.5	25
$T_R$ [a.u.]	2	1	2	2	2
$\tau_{\text{decay}}$ [a.u.]	48.8	47.7	42.1	31.2	14.5

**Table S1.** Fitted decay times of noiseless simulated data under the influence of different RF schemes (compare Fig. S6). Assumed experimental parameters without pulses:  $P_0 = 0.3$ ,  $\tau_{\text{decay}} = 50$

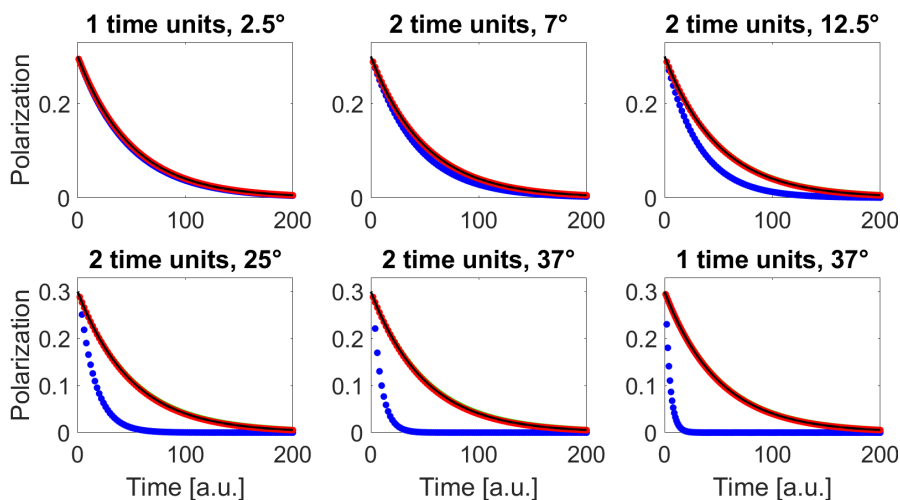


**Fig. S7.** The exact correction scheme works well for a large range of RF schemes. The ground truth data (without RF pulses) is shown in black. Simulation with RF pulses before and after iterative correction are shown in blue and red, respectively. The  $\cos^{-n}$  corrected data is shown in green but not visible as it works equally good as the iterative correction such that the two overlay. Assumed experimental parameters without pulses:  $P_0 = 0.3$ ,  $\tau_{\text{decay}} = 50$

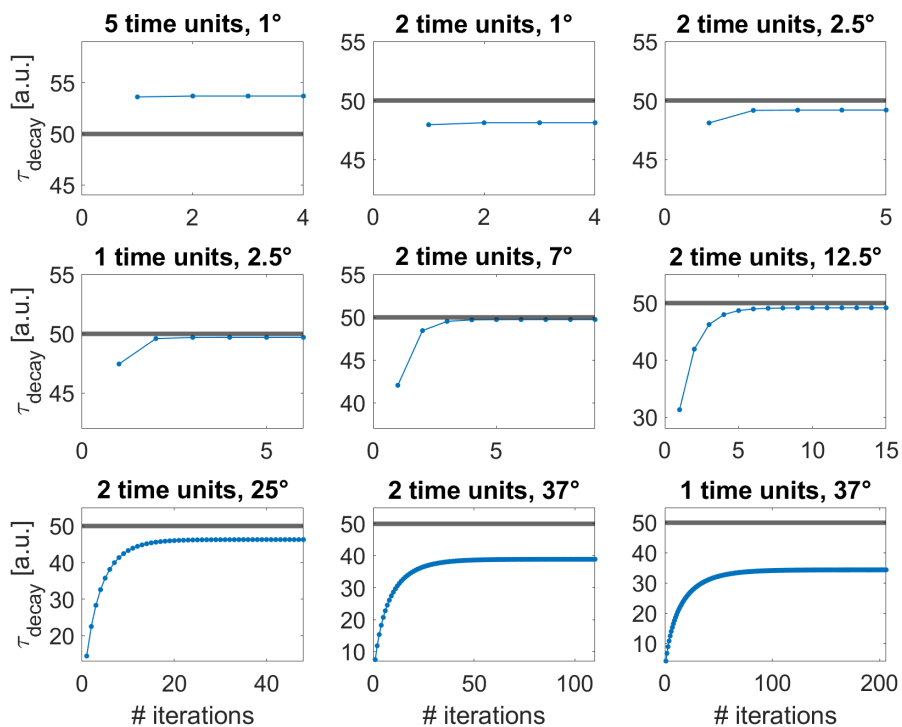


**Fig. S8.** Simulating the convergence of  $\tau_{\text{decay}}$  in the self-consistent algorithm for synthetic experimental (noisy) data for different RF pulse settings. Assumed experimental parameters without pulses:  $P_0 = 0.3$ ,  $\tau_{\text{decay}} = 50$ , maximum of 500 self-consistent iteration steps

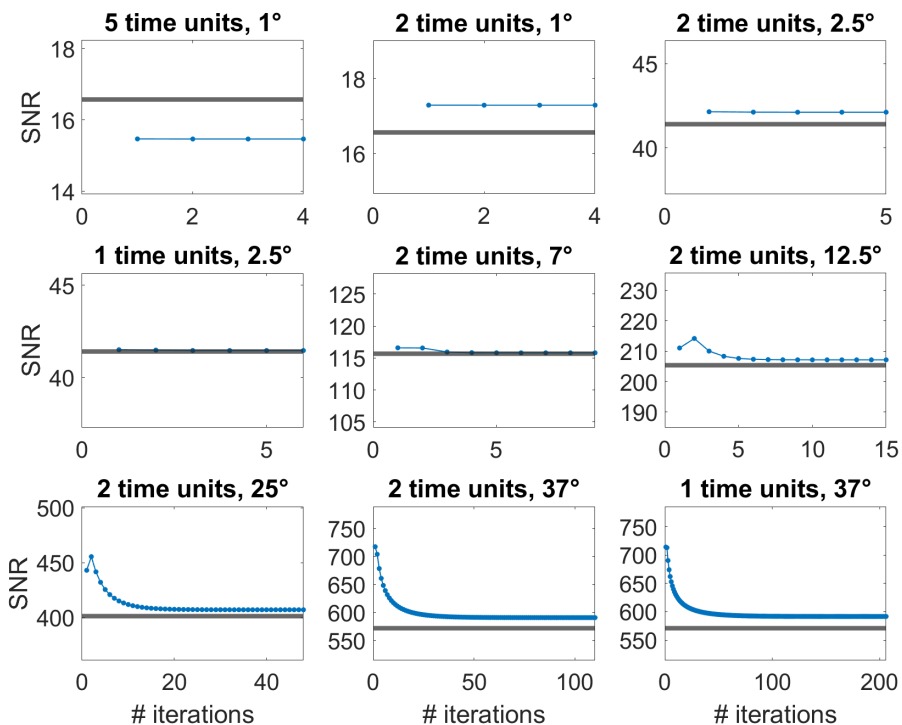


**Fig. S9.** Simulating the convergence of the SNR and with it the polarization in the self-consistent algorithm for synthetic experimental (noisy) data for different RF pulse settings. Assumed experimental parameters without pulses:  $P_0 = 0.3$ ,  $\tau_{\text{decay}} = 50$ , maximum of 500 self-consistent iteration steps

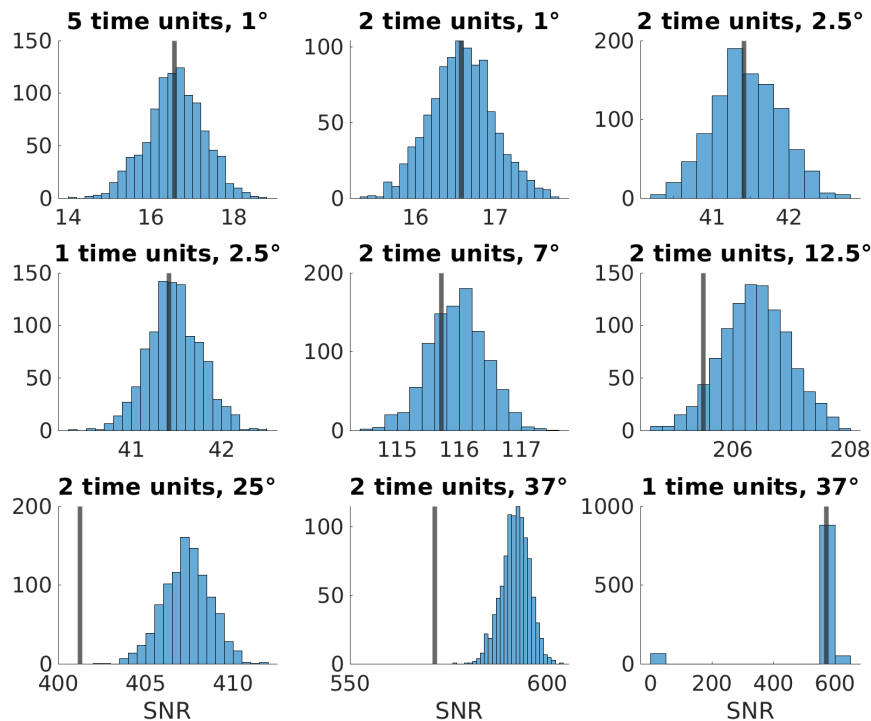


**Fig. S10.** Results of the iterative self-consistent correction algorithm for the SNR with different RF schemes. Assumed experimental parameters without pulses:  $P_0 = 0.3$ ,  $\tau_{\text{decay}} = 50$ , maximum of 500 self-consistent iteration steps, 1000 configurations. The results with zero SNR refer to cases in which the algorithm could not find a self-consistent solution for the given convergence criterion (less than  $10^{-4}$  time units difference for the time constant between consecutive iteration steps).

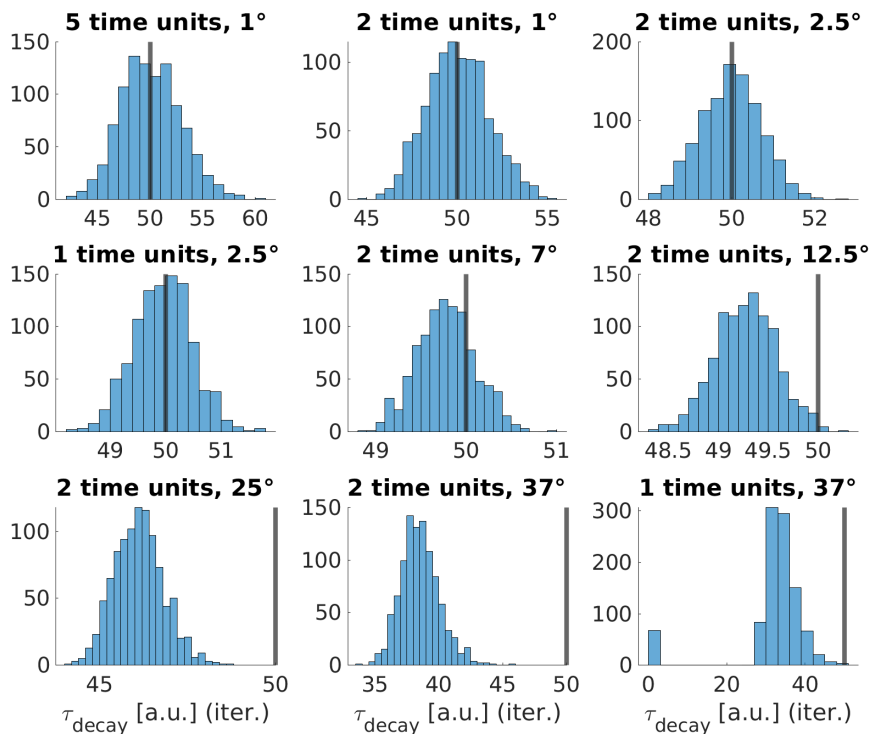


**Fig. S11.** Results of the iterative self-consistent correction algorithm for the decay time constants with different RF schemes. Assumed experimental parameters without pulses:  $P_0 = 0.3$ ,  $\tau_{\text{decay}} = 50$ , maximum of 500 self-consistent iteration steps, 1000 configurations. The results with zero decay time refer to cases in which the algorithm could not find a self-consistent solution for the given convergence criterion (less than  $10^{-4}$  time units difference for the time constant between consecutive iteration steps).

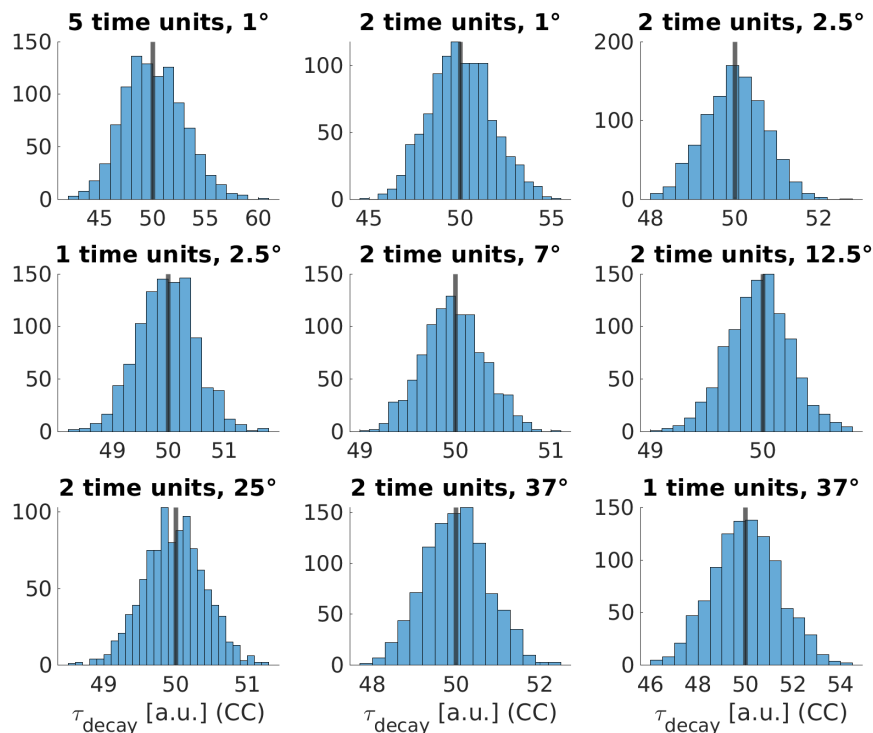


**Fig. S12.** Results of decay time correction introduced in [1] (CC model). Assumed experimental parameters without pulses:  $P_0 = 0.3$ ,  $\tau_{\text{decay}} = 50$ , 1000 configurations.

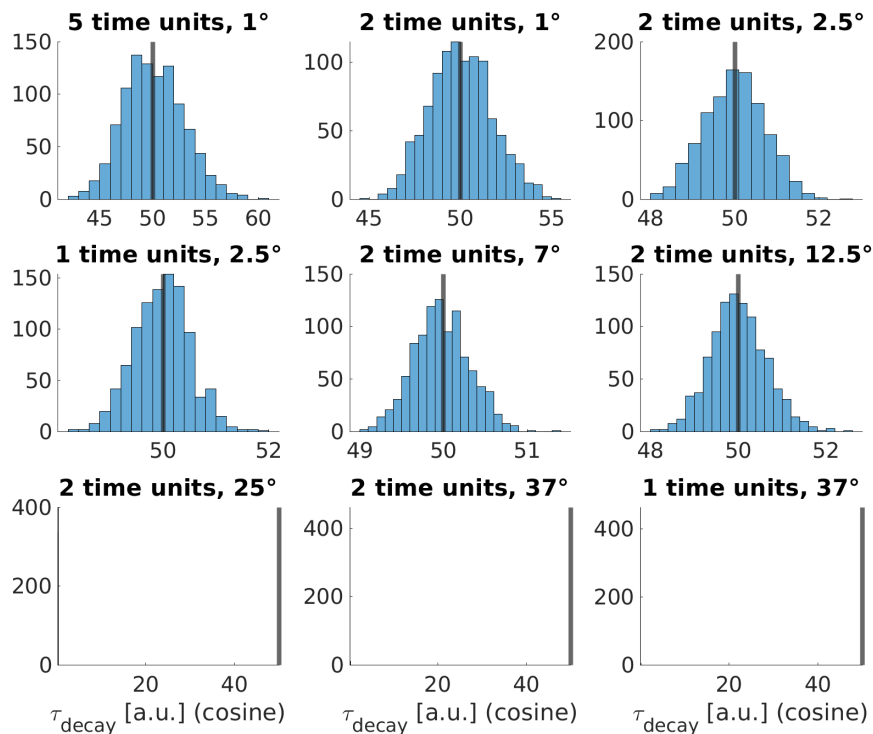


**Fig. S13.** Simple  $\cos^{-n}$  correction. Assumed experimental parameters without pulses:  $P_0 = 0.3$ ,  $\tau_{\text{decay}} = 50$ , 1000 configurations. For the stronger RF pulse schemes, this correction amplifies the small but finite noise with the divergent correction factor preventing a reasonable fit.

### S3 Experimental signal

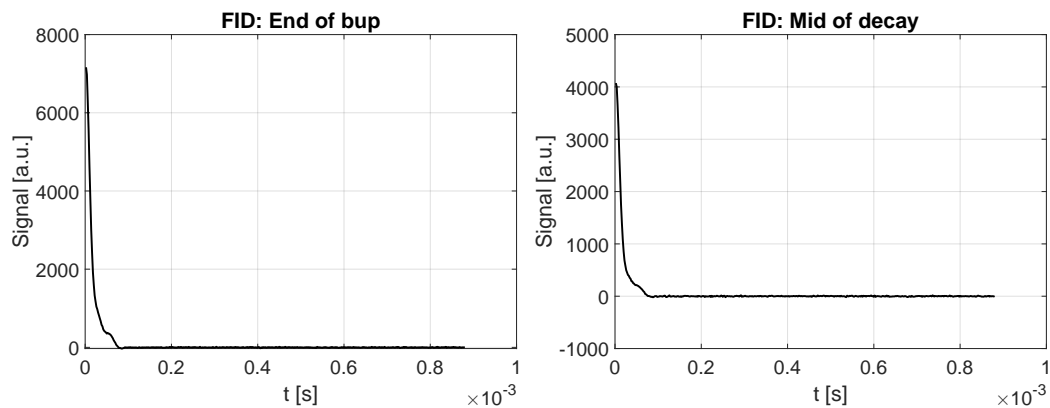


**Fig. S14.** 2.4° experimental (uncorrected) data for 4-oxo-TEMPO in natural abundance water/glycerol (1/1)<sub>v</sub>. The SNR based on the signal of the first data point compared to the standard deviation of the last 100 points of the FID (no apodization) is 1140 despite a long prescan delay of 18  $\mu$ s and the short  $T_2^*$  due to the high proton concentration.

### References

- [1] Andrea Capozzi, Tian Cheng, Giovanni Boero, Christophe Roussel, and Arnaud Comment. Thermal annihilation of photo-induced radicals following dynamic nuclear polarization to produce transportable frozen hyperpolarized <sup>13</sup>C-substrates. *Nature Communications*, 8:1–7, 2017.